Journal of Heat Transfer

Technical Brief

Optimally Staggered Finned Circular and Elliptic Tubes in Turbulent Forced Convection

R. L. S. Mainardes

R. S. Matos

J. V. C. Vargas[1]
e-mail: jvargas@demec.ufpr.br

Departamento de Engenharia Mecânica,
Centro Politécnico,
Universidade Federal do Paraná,
Caixa Postal 19011,
Curitiba, PR, 81531-990, Brazil

J. C. Ordonez
Departament of Mechanical Engineering and Center for Advanced Power Systems,
Florida State University,
Tallahassee, FL, 32310-6046

This work presents an experimental geometric optimization study to maximize the total heat transfer rate between a bundle of finned tubes in a given volume and a given external flow both for circular and elliptic arrangements, for general staggered configurations. The results are reported for air as the external fluid, in the range $2650 \leq \mathrm{Re}_{2b} \leq 10{,}600$*, where* $2b$ *is the smaller ellipse axis. Experimental optimization results for finned circular and elliptic tubes arrangements are presented. A relative heat transfer gain of up to 80%* ($\mathrm{Re}_{2b}=10{,}600$) *is observed in the elliptic arrangement optimized with respect to tube-to-tube spacings, as compared to the optimal circular one. A relative heat transfer gain of 80% is observed in the three-way optimized elliptic arrangement in comparison with the two-way optimized circular one; i.e., with respect to tube-to-tube and fin-to-fin spacings. An empirical correlation for the three-way optimized configuration was obtained to evaluate the resulting maximized dimensionless heat transfer rate.* [DOI: 10.1115/1.2712860]

Keywords: heat transfer enhancement, constructal theory, internal geometry

[1]Corresponding author.

Contributed by the Heat Transfer Division of ASME for publication in the Journal of Heat Transfer. Manuscript received April 10, 2006; final manuscript received December 15, 2006. Review conducted by Anthony M. Jacobi.

1 Introduction

Finned cross-flow heat exchangers are part of numerous engineering processes in industry and are unquestionably responsible for a large share of the total energy consumption wherever they are present [1–12].

In this work, the geometric optimization of design parameters for maximum heat transfer is pursued experimentally. The basic idea is to analyze the heat transfer gain using elliptic tubes heat exchangers as compared to the traditional circular ones when varying the following design parameters: δ=fin-to-fin spacing; e =ellipses' eccentricity, and S=spacing between rows of tubes. Hence, the problem consists of identifying a configuration (internal architecture, shape) that provides maximum heat transfer for a given space [13].

The paper describes a series of experiments conducted in the laboratory in the search for optimal geometric parameters in general staggered finned circular and elliptic configurations for maximum heat transfer in turbulent flow. Circular and elliptic arrangements, with the same flow obstruction cross-sectional area, are then compared on the basis of maximum total heat transfer and total mass of manufacturing material.

2 Theory

Dimensionless variables have been defined based on appropriate physical scales as follows

$$\theta = \frac{T - T_\infty}{T_w - T_\infty} \qquad \mathrm{Re}_{2b} = \frac{u_\infty (2b)}{\nu} \tag{1}$$

The dimensionless overall thermal conductance $\tilde{q}$, or volumetric heat transfer density, is defined as follows [14–16]

$$\tilde{q} = \frac{Q/(T_w - T_\infty)}{kLHW/(2b)^2} \tag{2}$$

where the overall heat transfer rate between the finned tubes and the free stream, i.e., Q, has been divided by the constrained volume, LHW; k is the fluid thermal conductivity [W m^{-1} K^{-1}], and $2b=D$ the ellipse smaller axis or tube diameter.

A balance of energy in one elemental channel states that

$$Q = N_{\mathrm{ec}} Q_{\mathrm{ec}} = N_{\mathrm{ec}} \dot{m}_{\mathrm{ec}} c_p (\bar{T}_{\mathrm{out}} - T_\infty) \tag{3}$$

where N_{ec} is the number of elemental channels. The elemental channel is defined as the sum of all unit cells in direction z. Therefore, the mass flow rate [kg s^{-1}] entering one elemental channel is

$$\dot{m}_{\mathrm{ec}} = \rho u_\infty [(S + 2b)/2](W - n_f t_f) \tag{4}$$

The number of fins in the arrangement is given by

$$n_f = \frac{W}{t_f + \delta} \tag{5}$$

The dimensionless overall thermal conductance is rewritten utilizing Eqs. (2)–(5) as follows

$$\tilde{q} = \frac{N_{ec}}{2}\Pr \mathrm{Re}_{2b}\left[\frac{2b}{L}\right]^2 \frac{2b}{H}\left(\frac{S}{2b}+1\right)(1-\phi_f)\bar{\theta}_{out} \tag{6}$$

where $\phi_f = n_f t_f / W = t_f / t_f + \delta$, is the dimensionless linear fin density $(0 \leqslant n_f t_f \leqslant W)$, and Pr the fluid Prandtl number; i.e., ν/α.

For the sake of generalizing the results for all configurations of the type studied in this work, the dimensionless overall thermal conductance is alternatively defined as follows

$$\tilde{q}_* = \frac{2}{N_{ec}}\left[\frac{L}{2b}\right]^2 \frac{H}{2b}\tilde{q} = \Pr \mathrm{Re}_{2b}\left(\frac{S}{2b}+1\right)(1-\phi_f)\bar{\theta}_{out} \tag{7}$$

The volume fraction occupied by solid material in the arrangement is given by

$$\tilde{V} = \frac{W}{L^3}\{n_t\pi[ab-(a-t_t)(b-t_t)] + \phi_f(LH - n_t\pi ab)\} \tag{8}$$

where t_t is the thickness of the tube wall (m) and n_t is the total number tubes of the arrangement.

3 Experiments

The same experimental rig that was utilized in previous studies for the laminar regime [14–16] was re-utilized in the laboratory to produce the necessary experimental data to perform the experimental optimization of finned arrangements. The forced air flow was induced by suction with an axial electric fan, with a nominal power of 1 HP, and was capable of providing air free-stream velocities (u_∞) up to 20 m s^{-1}.

The objective of the experimental work was to evaluate the volumetric heat transfer density (or overall thermal conductance) of each tested arrangement by computing $\tilde{q}_*$ with Eq. (7) through direct measurements of $u_\infty(\mathrm{Re}_{2b})$, and $\bar{T}_{out}$, $\bar{T}_W$, and $T_\infty(\bar{\theta}_{out})$. The volume fraction occupied by solid material in the arrangement, i.e., $\tilde{V}$, was also evaluated according to Eq. (8), in order to compare the resulting total volume of solid material of the elliptic and circular arrangements.

Five runs were conducted for each experiment. Steady-state conditions were reached after 3 h in all the experiments. The precision limit for each temperature point was computed as two times the standard deviation of the five runs [17]. It was verified that the precision limits of all variables involved in the calculation of $\tilde{q}_*$ were negligible in comparison to the precision limit of $\bar{\theta}_{out}$, therefore $P_{\tilde{q}_*} = P_{\bar{\theta}_{out}}$. The thermistors, anemometer, properties, and lengths bias limits were found negligible in comparison with the precision limit of $\tilde{q}_*$. As a result, the uncertainty of $\tilde{q}_*$ was calculated by

$$\frac{U_{\tilde{q}_*}}{\tilde{q}_*} = \left[\left(\frac{P_{\tilde{q}_*}}{\tilde{q}_*}\right)^2 + \left(\frac{B_{\tilde{q}_*}}{\tilde{q}_*}\right)^2\right]^{1/2} \cong \frac{P_{\bar{\theta}_{out}}}{\bar{\theta}_{out}} \tag{9}$$

Several free-stream velocities; set points were tested, such that $u_\infty = 2.5$, 5.0, 7.5, and 10.0 m s^{-1}, corresponding to $\mathrm{Re}_{2b} = 2650$, 5300, 7950, and 10,600, respectively, which covered a significant portion of the air velocity range of interest for typical air conditioning applications; i.e., 1.8 m s$^{-1} \leqslant u_\infty \leqslant 18.2$ m s^{-1} [2]. For those values of Re_{2b}, the turbulent flow regime is observed. The largest uncertainty calculated according to Eq. (10) in all tests was $U_{\tilde{q}_*}/\tilde{q}_* = 0.075$.

4 Results and Discussion

For each tested Reynolds number (Re_{2b}), the three-way optimization procedure was performed according to the following steps: (i) for a given eccentricity, the dimensionless overall thermal conductance $\tilde{q}_*$ was computed with Eq. (7), for the range of tube-to-tube spacings $0.1 \leqslant S/2b \leqslant 1.5$; (ii) the same procedure was repeated for several eccentricities, i.e., $e = 0.4$, 0.5, 0.6, and 1; and (iii) steps (i) and (ii) were repeated for different fin-to-fin spacings configurations; i.e., $\phi_f = 0.006$, 0.094, and 0.26.

This study presents experimental optimization results for a higher range of Reynolds numbers than in previous optimization studies for finned elliptic tubes arrays [15,16], i.e., for $\mathrm{Re}_{2b} = 2650$, 5300, 7950, and 10,600, therefore investigating the turbulent flow regime.

The first step of the three-way optimization procedure is documented by Figs. 1(*a*)–1(*c*), which show the experimental optimization of the same tube-to-tube spacing, $S/2b$, for $e = 1$, 0.6, and 0.5, respectively, for a fixed fin-to-fin spacing $\phi_f = 0.006$. It is observed that the maximum is less pronounced for lower values of Re_{2b}. This phenomenon is physically expected based on the fact that heat transfer increases as mass flow rate increases.

The experiments have shown that $(S/2b, e)_{opt} \cong (0.5, 0.6)$ for $\phi_f = 0.006$. Indeed, Fig. 2 depicts the one-way maximized $\tilde{q}_{*,m}$ values obtained experimentally for $0.5 \leqslant e \leqslant 1$, for a fixed fin-to-fin spacing $\phi_f = 0.006$. As Re_{2b} increases, the importance of optimal design is noticeable as turbulence takes place.

Figure 3(*a*) illustrates the existence of a local optimal fin-to-fin spacing, (ϕ_f) for $(S/2b)_{opt} = 0.5$ and $e = 1$ (circular tubes). Figure 3(*b*) reports the results of the three-way global optimization with respect to the three degrees of freedom, $S/2b$, e, and ϕ_f, obtained after performing the three steps of the optimization procedure. The geometric parameters were determined experimentally such that $\tilde{q}_*$ was maximized three times; i.e., $(S/2b, e, \phi_f)_{opt} \cong (0.5, 0.6, 0.094)$. The three-way optimized internal configuration is "robust" with respect to the variation of the Reynolds number. A correlation for $2650 \leqslant \mathrm{Re}_{2b} \leqslant 10{,}600$ is given by

$$\tilde{q}_{*,mmm} = 2943.8 - 0.16778\,\mathrm{Re}_{2b} + 0.00019174\,\mathrm{Re}_{2b}^2 \qquad R = 0.9978 \tag{10}$$

Figure 4 shows the experimentally determined points for $\tilde{q}_{*,mmm}$, and a curve plotted with Eq. (10). The $\tilde{q}_{*,mmm}$ trend with respect to the variation of Re_{2b} is well approximated.

In sum, a heat transfer gain of up to 80% was observed in the three-way optimized elliptic arrangement of Fig. 3(*b*), as compared to the two-way optimized circular one.

Figure 5 shows the volume fraction of solid material computed with Eq. (9). When the dimensionless fin density is small, the volume fraction of solid material $(\tilde{V})$ increases as eccentricity decreases (from 0.033 at $e = 1$ to 0.053 at $e = 0.4$, for $\phi_f = 0.006$). Such trend is inverted as the number of fins increases. For example, the volume fraction $\tilde{V} \cong 0.104$ for $e = 0.5$, 0.6, and 1, for $\phi_f = 0.094$, and $\tilde{V} = 0.215$, 0.222, and 0.238 for $e = 0.5$, 0.6, and 1, respectively, for $\phi_f = 0.26$, as is shown by Fig. 5. Thus, for the three-way optimized elliptic configuration, with $\phi_{f,opt} = 0.094$, the volume fraction of solid material of the elliptic arrangement is the same as the circular one. Therefore, the same amount of material is required for manufacturing both the three-way optimized elliptic arrangement and the circular one with the same dimensionless fin density.

5 Conclusions

Several experimental arrangements were built in the laboratory and many test runs were conducted in a wind tunnel in turbulent forced convection. The internal geometric structure of the arrangements was optimized for maximum heat transfer. Better global performance is achieved when flow and heat transfer resistances are minimized together. Optimal distribution of imperfection represents flow architecture, or constructal design [13].

A comparison criterion was adopted as in previous studies [1–3,14–16], i.e., establishing the same air input velocity and flow obstruction cross-sectional for the circular and elliptic arrangements, to compare the arrangements on the basis of maximum heat transfer in the most isolated way possible. An optimal set of

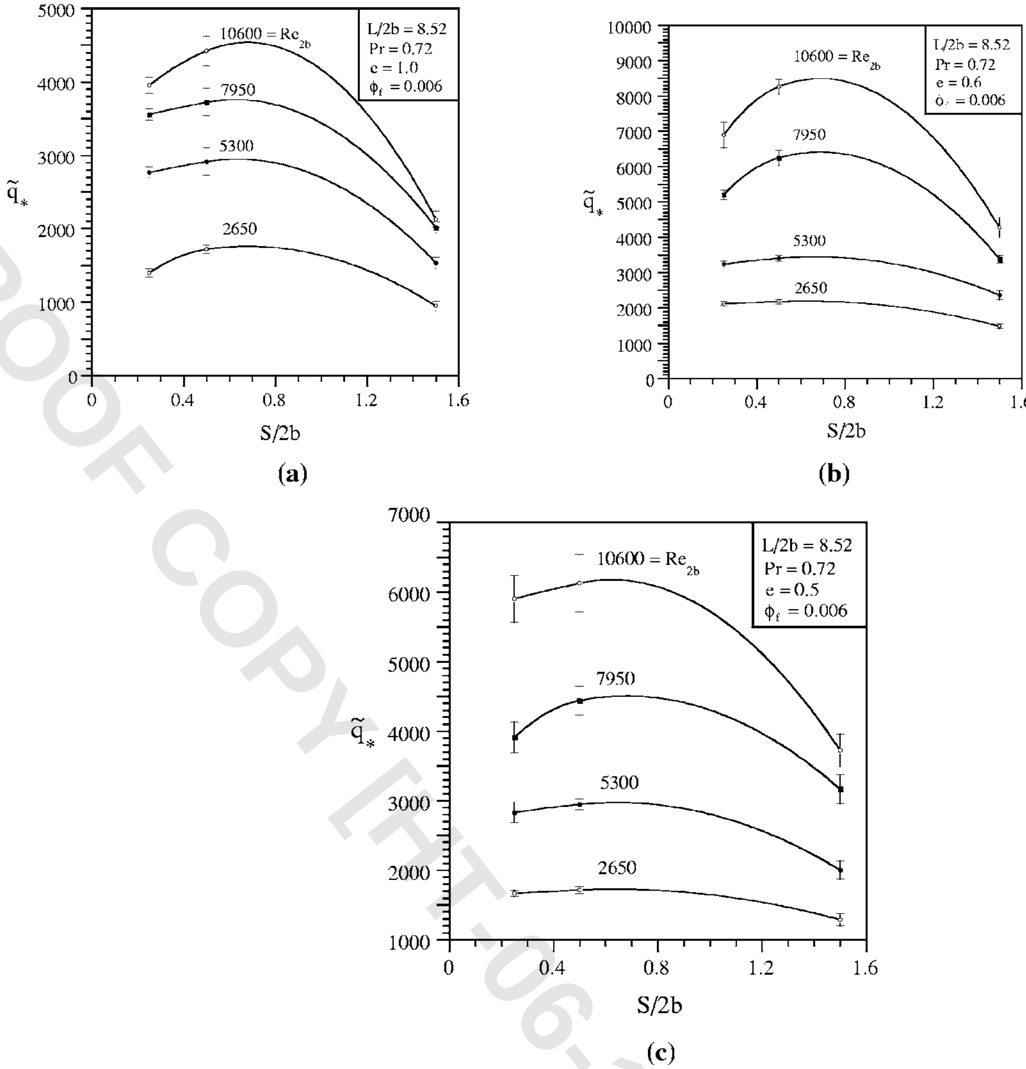

Fig. 1 (***a***) **One-way experimental optimization results (*e*=1 and Re_{2b}=2650, 5300, 7950, and 10,600); (*b*) one-way experimental optimization results (*e*=0.6 and Re_{2b}=2650, 5300, 7950, and 10,600), and (c) one-way experimental optimization results (*e*=0.5 and Re_{2b}=2650, 5300, 7950, and 10,600)**

geometric parameters was determined experimentally such that $\tilde{q}_*$ was maximized three times, i.e., $(S/2b, e, \phi_f)_{\mathrm{opt}} \cong (0.5, 0.6, 0.094)$, where the three-way maximized dimensionless heat transfer rate is

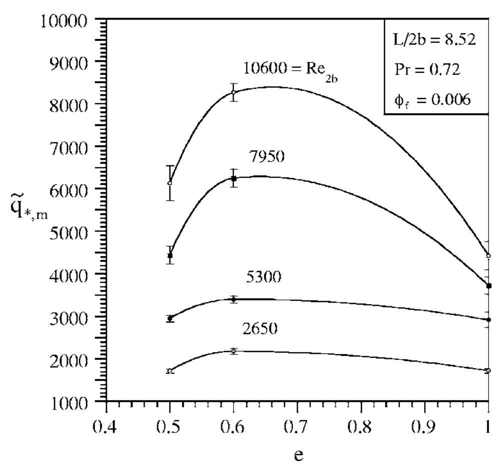

Fig. 2 Two-way optimization of finned arrangements with respect to tube-to-tube spacing and eccentricity

achieved. The three-way optimized elliptic arrangement exhibits a heat transfer gain of up to 90% relative to the optimal circular tube arrangement. A compact analytical correlation was proposed to estimate the actual three-way maximized heat transfer rate in the design of elliptic tubes heat exchangers of the type studied in this paper. For the three-way optimized elliptic configuration, with $\phi_{f,\mathrm{opt}}$=0.094, the volume fraction of solid material of the elliptic arrangement is the same as the circular one. The heat transfer gain, and a similar amount of material to manufacture both arrangements show that the elliptic tubes optimized arrangement has the potential to deliver significantly higher global performance than the circular arrangement, with a similar investment cost.

Nomenclature

- a = larger ellipse semi-axis, m
- b = smaller ellipse semi-axis, m
- B_a = bias limit of quantity a
- c_p = fluid specific heat at constant pressure, J kg^{-1} K^{-1}
- D = tube diameter, m
- e = ellipses eccentricity: b/a
- H = array height, m
- k = fluid thermal conductivity, W m^{-1} K^{-1}

PROOF COPY [HT-06-1163] 018705JHR

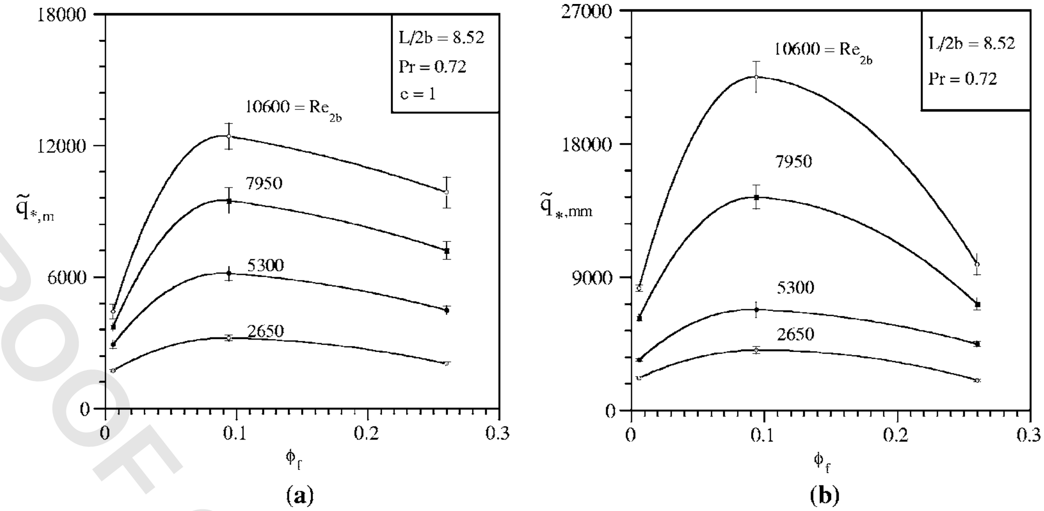

Fig. 3 (*a*) **Two-way optimization of finned circular arrangements with respect to tube-to-tube and fin-to-fin spacing, and (*b*) three-way optimization of finned arrangements with respect to tube-to-tube spacing, eccentricity and fin-to-fin spacing.**

L = array length, m
$L/2b$ = array length to smaller ellipses axis aspect ratio
$\dot{m}_{ec}$ = fluid mass flow rate entering one elemental channel, kg s^{-1}
n_f = number of fins
n_t = total number of tubes in the arrangement
N = number of tubes in one unit cell
N_{ec} = number of elemental channels
t_f = fin thickness, m
t_t = tube thickness, m
T = temperature, K
$\overline{T}$ = average fluid temperature, K
Pr = fluid Prandtl number: ν/α
P_a = precision limit of quantity a
$\tilde{q}$ = dimensionless overall thermal conductance, Eq. (2)
$\tilde{q}_*$ = dimensionless overall thermal conductance, Eq. (7)
Q = overall heat transfer rate, W
Q_{ec} = heat transfer rate of one elemental channel, W
R = statistics correlation coefficient
Re_{2b} = Reynolds number based on smaller ellipse semi-axis length: $u_\infty(2b)/\nu$
S = spacing between rows of tubes, m
S/D = dimensionless spacing between rows of tubes (circular arrangement)
$S/2b$ = dimensionless spacing between rows of tubes (elliptic arrangement)
U_a = uncertainty of quantity a
$\tilde{V}$ = volume fraction, Eq. (8)
W = array width, m

Greek Symbols

α = thermal diffusivity, m^2/s
δ = fin-to-fin spacing, m
θ = dimensionless temperature
$\overline{\theta}$ = dimensionless average fluid temperature
ν = fluid kinematic viscosity, m^2 s^{-1}
ρ = density, kg m^{-3}
ϕ_f = dimensionless fin density in direction z

Subscripts

m = 1-way maximum

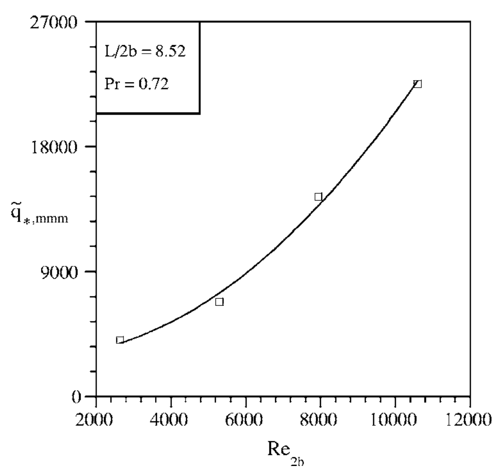

Fig. 4 The three-way maximized dimensionless heat transfer rate with respect to Re$_{2b}$

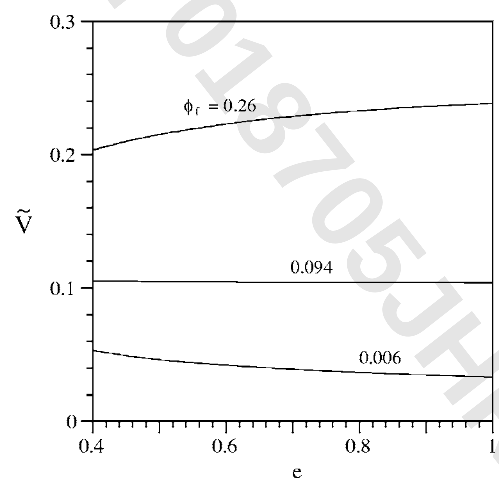

Fig. 5 The total solid volume fraction of the arrangements with respect to eccentricity and fin-to-fin spacing

mm = 2-way maximum
mmm = 3-way maximum
opt = optimal
out = unit cell outlet
w = tube surface
∞ = free-stream

References

[1] Bordalo, S. N., and Saboya, F. E. M., 1999, “Pressure Drop Coefficients for Elliptic and Circular Sections in One, Two and Three-Row Arrangements of Plate Fin and Tube Heat Exchangers,” J. Braz. Soc. Mech. Sci., **21**(4) pp. 600–610.

[2] Saboya, S. M., and Saboya, F. E. M., 2001, “Experiments on Elliptic Sections in One and Two-Row Arrangements of Plate Fin and Tube Heat Exchangers,” Exp. Therm. Fluid Sci., **24**(1–2), pp. 67–75.

[3] Rosman, E. C., Carajilescov, P., and Saboya, F. E. M., 1984, “Performance of One and Two-Row Tube and Plate Fin Heat Exchangers,” ASME J. Heat Transfer, **106**(3), pp. 627–632.

[4] Khan, M. G., Fartaj, A., and Ting, D. S. K., 2004, “An Experimental Characterization of Cross-Flow Cooling of Air via an In-Line Elliptical Tube Array,” Int. J. Heat Fluid Flow, **25**(4), pp. 636–648.

[5] Elshazly, K., Moawed, M., Ibrahim, E., and Emara, M., 2005, “Heat Transfer by Free Convection from the Inside Surface of the Vertical and Inclined Elliptic Tube,” Energy Convers. Manage., **46**(9–10), pp. 1443–1463.

[6] Elsayed, A. O., Ibrahim, E. Z., and Elsayed, S. A., 2003, “Free Convection from a Constant Heat Flux Elliptic Tube,” Energy Convers. Manage., **44**(15), pp. 2445–2453.

[7] Min, J. C., and Webb, R. L., 2004, “Numerical Analyses of Effects of Tube Shape on Performance of a Finned Tube Heat Exchanger,” J. Enhanced Heat Transfer, **11**(1), pp. 61–73.

[8] Kundu, B., Maiti, B., and Das, P. K., 2006, “Performance Analysis of Plate Fins Circumscribing Elliptic Tubes,” Heat Transfer Eng., **27**(3), pp. 86–94.

[9] O’Brien, J. E., and Sohal, M. S., 2005, “Heat Transfer Enhancement for Finned-Tube Heat Exchangers With Winglets,” ASME J. Heat Transfer, **127**(2), pp. 171–178.

[10] O’Brien, J. E., Sohal, M. S., and Wallstedt, P. C., 2004, “Local Heat Transfer and Pressure Drop for Finned-Tube Heat Exchangers Using Oval Tubes and Vortex Generators,” ASME J. Heat Transfer, **126**(5), pp. 826–835.

[11] Gao, S. D., Wang, L. B., Zhang, Y. H., and Ke, F., 2003, “The Optimum Height of Winglet Vortex Generators Mounted on Three-row Flat Tube Bank Fin,” ASME J. Heat Transfer, **125**(6), pp. 1007–1016.

[12] Kim, N. H., Youn, B., and Webb, R. L., 1999, “Air-Side Float Transfer and Friction Correlations for Plain Fin-and-Tube Heat Exchangers With Staggered Tube Arrangements,” ASME J. Heat Transfer, **121**(3), pp. 662–667.

[13] Bejan, A., 2000, *Shape and Structure, From Engineering to Nature*, Cambridge University Press, Cambridge, UK.

[14] Matos, R. S., Vargas, J. V. C., Laursen, T. A., and Saboya, F. E. M., 2001, “Optimization Study and Heat Transfer Comparison of Staggered Circular and Elliptic Tubes in Forced Convection,” Int. J. Heat Mass Transfer, **44**(20), pp. 3953–3961.

[15] Matos, R. S., Vargas, J. V. C., Laursen, T. A., and Bejan, A., 2004, “Optimally Staggered Finned Circular and Elliptic Tubes in Forced Convection,” Int. J. Heat Mass Transfer, **47**(6–7), pp. 1347–1359.

[16] Matos, R. S., Laursen, T. A., Vargas, J. V. C., and Bejan, A., 2004, “Three-Dimensional Optimization of Staggered Finned Circular and Elliptic Tubes in Forced Convection,” Int. J. Therm. Sci., **43**(5), pp. 477–487.

[17] Editorial, 1993, “Journal of Heat Transfer Policy on Reporting Uncertainties in Experimental Measurements and Results,” ASME J. Heat Transfer, **115**, pp. 5–6.